An arylthiazyne derivative is a potent inhibitor of lipid peroxidation and ferroptosis providing neuroprotection in vitro and in vivo

Keuters, Meike Hedwig

2021-02-10

Keuters , M H , Keksa-Goldsteine , V , Dhungana , H , Huuskonen , M T , Pomeshchik , Y , Savchenko , E , Korhonen , P K , Singh , Y , Wojciechowski , S , Lehtonen , S , Kanninen , K M , Malm , T , Sirviö , J , Muona , A , Koistinaho , M , Goldsteins , G & Koistinaho , J 2021 , ' An arylthiazyne derivative is a potent inhibitor of lipid peroxidation and ferroptosis providing neuroprotection in vitro and in vivo ' , Scientific Reports , vol. 11 , no. 1 , 3518 . https://doi.org/10.1038/s41598-021-8

http://hdl.handle.net/10138/334982
https://doi.org/10.1038/s41598-021-81741-3

scientific reports

Check for updates

• ƒ ”› Ž – Š ‹ ƒ œ › • ‡ † ‡ ” ‹ ˜ ƒ – ‹ • ƒ ’ ‘ – ‡ • – ‹ • Š ‹ „ ‹ – ‘ ” ‘ ^ Ž ’ ‡ ” ‘ š ‹ † ƒ – ‹ ‘ • ƒ • † ^ ‡ ” ” ‘ ’ – ‘ • ’ ” ‘ ˜ ‹ † ‹ • ‰ • ‡ — ” ‘ ’ ” ‘ – ‡ … – ‹ ƒ • † ‹ • ˜ ‹ ˜ ‘

‡ ‹ • ‡ ‡ † ™ ‹ ‰ ʷ á å — ‡ Ž – ƒ ‡ • • ƒ æ ʷ á Ž † ‹ • ” ƒ ‡ ƒ • ‡ Š — ʷ á å ‰ ƒ • ƒ
‹ • • ‘ ä — — • ʷ á • ‡ • — ” ‹ › ‘ • ‡ ʷ á Š … • Š ƒ ↔ ‡ ” ƒ ‹ ˜ ƒ .. Š ‡ ʷ á • ‘ ƒ — Ž ƒ ä ʷ á ” Š ‘ • ‡ •
ƒ Œ — ˜ ‹ • † ‰ ‰ á Š ƒ ” ‘ ƒ Œ … ‹ ‡ … Š á ‘ ™ ž ˘ • ƒ ‡ Š ʷ á ‘ • ‡ ƒ • — Œ ƒ ä ʷ á • • ‹ • ‡ •
ƒ ” Œ ƒ ʷ á Ž • — • ” ‹ ˜ ˇ á Ú • — ˣ á • ƒ ‹ Ž Ž ƒ ‘ ‹ ˇ á ‹ • ƒ Š † ƒ Ž † • – ‡ ʷ ‹ • •
ƒ ” ‹ ‘ ‹ • – ʷ ˇ • ƒ Š ‘

‹ ’ ‹ † ’ ‡ ” ‘ š ‹ † ƒ – ‹ ‘ • æ ‹ • ‹ – ‹ ƒ – ‡ † ^ ‡ ” ” ‘ ’ – ‘ • ‹ • ‹ • ƒ • ‹ • ‡ … Š ƒ • ‹ •
– ƒ • ‹ • ‰ ’ Ž ƒ … ‡ ‹ • • ‡ — ” ‘ Ž ‘ ‰ ‹ … ƒ Ž † ‹ • ‡ ƒ • ‡ • ä ‡ ” ‡ ™ ‡ • Š ‘ ™ – Š ƒ – ƒ … ‘ • †
• • ƒ Ž Ž • ‘ Ž ‡ … — Ž ‡ ™ ‹ – Š ƒ • ƒ ” › Ž – Š ‹ ƒ œ ‹ • ‡ „ ƒ tent • æ ‘ – ‡ – › Ž Š æ z v ” • ‘ æ † v ” { ˇ ‹ † ‡ Š ‹ „
æ ‹ • † — … ‡ † Ž ‹ ’ ‹ † ’ ‡ ” ‘ š ‹ † ƒ – ‹ ‘ • ƒ • † ’ ” ‘ – ‡ … – • ƒ ‰ ƒ ‹ • • – ^ ‡ ” ” ‘ ’ – ‘ –
‰ Ž — – ƒ – Š ‹ ‘ • ‡ † ‡ ’ Ž ‡ – ‹ ‘ • ‘ ” ‰ Ž — – ƒ – Š ‹ ‘ • ‡ ’ ‡ ” ‘ š ‹ † ƒ • ‡ z š z ‹ • Š ‹ „
ƒ † † ‹ – ‹ ‘ • á æ z v • æ v { x • — ’ ” ‡ • • ‡ • ’ ” ‘ æ ‹ • ª ƒ • • ƒ – ‘ ” › ƒ … – ‹ ˜ ƒ – ‹ ‘ • ‘ ^ x • ‹ •
• ‡ — ” ‘ • ƒ Ž … ‡ Ž Ž • ^ ” ‘ • … ‡ Ž Ž † ‡ ƒ – Š ‹ • † — … ‡ † „ › ’ ” ‘ æ ‹ • ª ƒ • • ƒ – ‘ ” › x | z ä
æ z v • æ v { x ‡ ¥ … ‹ ‡ • – Ž › ” ‡ † — … ‡ • ‹ • ^ ƒ ” … – ˜ ‘ Ž — • ‡ á ‡ † ‡ • ƒ ƒ • † ‡ š ’ ” ‡ • • ‹
‹ • ƒ • ‘ — • ‡ • ‘ † ‡ Ž ‘ ^ – Š ” ‘ • „ ‘ ‡ • „ ‘ Ž ‹ … • – ” ‘ • ‡ ä ƒ ” ‰ ‡ – ‹ • ‰ ^ ‡ ” ” ‘ ’ – ‘ • ‹ • • ƒ › ‹
• – ” ƒ – ‡ ‰ › ‹ • • ‡ — ” ‘ Ž ‘ ‰ ‹ … ƒ Ž † ‹ • ‡ ƒ • ‡ • ‹ • ˜ ‘ Ž ˜ ‹ • ‰ • ‡ ˜ ‡ ” ‡ • ‡ — ” ‘ • ƒ Ž † ‡ ƒ – Š

Abbreviations

Aif1	Allogra in ammatory factor 1
AD	Alzheimer's disease
AA	Arachidonic acid
Arg-1	Arginase-1
CCL2	Chemokine (C–C motif) ligand 2
COX-2	Cyclooxygenase-2
DAMPs	Damage-associated molecular patterns
Fe^{2+}/Fe^{3+}	Free iron (ferrous/ ferric iron)
GFAP	Glial brillary acidic protein
GSH	Glutathione
GPx4	Glutathione peroxidase 4
iFBS	(Heat-) inactivated fetal bovine serum
iNOS	Inducible nitric oxide synthase
IFN-	Interferon gamma
ICH	Intracerebral hemorrhage
i.p.	Intraperitoneal
Iba1	Ionized calcium-binding adapter molecule 1
LP	Lipid peroxidation
LPS	Lipopolysaccharide

ʷA.I. Virtanen Institute for Molecular Sciences, University of Eastern Finland, Kuopio, Finland. ˣAmanda Pharma Ltd., Kuopio, Finland. ʸ ‡ — ” ‘ • … ‹ ‡ • … ‡ ‡ • – ‡ ” á ‡ Ž • ‹ • • ‹ • • – ‹ – — – ‡ ‘ ^ ‹ ^ ‡ … | y á • … ‡ á
v v v w z ‡ Ž • ‹ • • ˇ á ‡ • ƒ • Ž Ž ƒ • ‹ Œ ƒ ” ‹ ä • ‘ ‹ • – ‹ • ƒ Š ‘ ; Š ‡ Ž • ‹ • • ‹ ä ¤

MFI	Median of the green uorescence intensity
MCA	Middle cerebral artery
MCP-1 (CCL2)	Monocyte chemotactic protein 1
NO	Nitric oxide
p.o.	Oral gavage/per os
PD	Parkinson's disease
PI	Propidium iodide
PTGS2	Prostaglandin-endoperoxide synthase 2
ROS	Reactive oxygen species
RNS	Reactive nitrogen species
s.e.m.	Standard error of the mean
TE model	romboembolic stroke model
TBHP	tert-Butyl hydroperoxide
TLR	Toll-like receptor
TNF-	Tumor necrosis factor alpha
tMCAO	Transient middle cerebral artery occlusion

Ferroptosis is an iron-dependent lipid peroxidation (LP) mechanism of non-apoptotic cell death[1]. It was recently discovered to be a major cell death pathway in neurodegenerative diseases, such as Parkinson's disease (PD), Alzheimer's disease (AD), and acute brain insults, including ischemic stroke and cerebral hemorrhage[2–7]. Upon injury, reactive oxygen species (ROS) and reactive nitrogen species (RNS) elevate free iron (Fe^{2+}/Fe^{3+}) concentration by interacting with proteins that regulate iron storage or release[8,9]. In turn, Fe^{2+}/Fe^{3+} decomposes H_2O_2 into harmful hydroxyl radicals ($HO^- + HO^{\bullet}$, thereby accelerating LP[8–10]. Fe^{2+}/Fe^{3+} also blocks regeneration of glutathione (GSH), the major cellular antioxidant. GSH is essential for the activity of the enzyme glutathione peroxidase 4 (GPx4) that is exclusively responsible for the reduction of cholesterol and phospholipid hydroperoxides and esteri ed oxidized fatty acids[11–13]. GSH depletion and inactivation of GPx4 are key initiators of ferroptosis[14]. Importantly, in severe neurological diseases, such as stroke, ferroptosis is coupled to neuroinammation by triggering the release of damage-associated molecular patterns (DAMPs), immunogenic lipid metabolites[15], and pro-in ammatory cytokines from activated immune cells[3,9,16]. While the activated immune cells release multiple pro-in ammatory factors, they simultaneously generate ROS, initiating another route for LP[17,18]. us, seemingly interdependent pathways of redox imbalance and in ammation facilitate each other and converge into mechanisms of neuronal damage.

Recently, two ferroptosis inhibitors, ferrostatin-1 and liproxstatin-1, were shown to be protective in mouse models of transient middle cerebral artery occlusion (tMCAO) and intracerebral hemorrhage (ICH)[18,20]. However, these two compounds poorly cross the blood–brain barrier[2,19] limiting their clinical development for brain diseases. Here we show that a condensed benzo[b]thiazine derivative with an arylthiazine backbone, ADA-409-052, inhibits ferroptotic cell death of neuronal cells through suppression of LP. e compound has a low molecular weight (MW: 330.33 g/mol), excellent calculated lipophilicity (Clog P of 2.31 (ideal log P value for passive di usion through the blood-brain barrier is 1.5–2.7[21,22]) and crosses well the blood-brain barrier in mice. Moreover, ADA-409-052 is strongly neuroprotective upon oral administration in a thromboembolic (TE) mouse model of stroke.

‡ • — Ž – •

æ z v • æ v { x ' " ‡ ˜ ‡ • – • Ž ‹ ' ‹ † ' ‡ " ' š ‹ † ƒ – ‹ ' • ‹ • † — PC-12 cells, exposed to 1 mM tert-Butyl hydroperoxide (TBHP), yielded massive LP, as shown by the increase of C11-BODIPY green uorescence signal (224.3% ± 59.1% when normalized to control; $p < 0.0001$, Fig. 1b). In contrast, the red uorescence signal remained predominant upon simultaneous treatment with ADA-409-052 (10 µM), which was comparable to control conditions (media only, Fig. 1a). Already the addition of ADA-409-052 at concentrations as low as of 0.625 µM suppressed some LP (to 183.7% ± 37.2%; Fig. 1d). Rising concentrations of ADA-409-052 up to 5–10 µM resulted in a potent dose-dependent reduction in TBHP-induced LP (1.25 µM: 161.1% ± 61.1%, 2.5 µM: 129.7% ± 43.5%, 5 µM: 124.5% ± 38.8%, 10 µM: 125.0% ± 49.3%; $p < 0.0001$; Fig. 1c). Flow cytometry analysis con rmed this reduction of TBHP-induced LP by ADA-409-052, showing a signi cantly lower median uorescent signal in TBHP-exposed (500 µM) PC-12 cells a er 10 µM ADA-409-052 treatment when compared with vehicle (green median uorescent intensity (MFI) of ADA-409-052/TBHP: 9.56 ± 1.1; MFI of TBHP only: 20.81 ± 5.3, $p = 0.0006$; Fig. 1e-f).

æ z v • æ v { x ' " ‡ ˜ ‡ • – • ^ ‡ " " ' ' – ' • ‹ • ‹ • † — … ‡ † „ ›Next, we tested ADA-409-052 •s e cacy against RSL3-induced ferroptosis in PC-12 cell cultures. e commercially available compound RSL3, a class II ferroptosis inducer, inactivates GPx4 causing ferroptotic cell death[23]. Figure 2a shows that 2.5 µM ADA-409-052 lowered RSL3-induced (0.25 µM) ferroptotic cell death signi cantly (ADA-409-052: 36.89% ± 2.21% cell viability compared to RSL3 only: 19.84% ± 1.44%; $p < 0.0001$). Adding 5 µM of ADA-409-052 rescued about 100% of the RSL3-treated cell population (ADA-409-052: 5 µM: 103.24% ± 3.12%, 10 µM: 102.39% ± 3.64%, 20 µM: 97.76% ± 1.39%; $p < 0.0001$). In comparison, our neuroprotective positive control compound, minocycline, was ine cient at concentrations below 10 µM and remained weak also at higher concentrations, although reaching signi cance (minocycline: 10 µM: 44.36% ± 3.6% cell viability, $p < 0.0001$; 20 µM: 53.87% ± 5.3% cell viability; $p < 0.0001$; Fig. 2b).

Figure 1. ADA-409-052 treatment protects PC-12 cells from TBHP-induced LP visualized with C11-BODIPY, a marker for cellular and intramembrane LP. (a–c) Representative, microscopic pictures of PC-12 cells exposed to (a) media control, (b) 1 mM TBHP, a class IV ferroptosis inducer, or (c) TBHP and ADA-409-052 (10 µM); scale bar: 100 µm. (d) Quantitative analysis of LP detected by a shi in the uorescence signal. Data normalized to control and displayed as percentage e.m.; = 3; One-way ANOVA with Tukey's multiple comparison test; ****p < 0.0001. (e) Flow cytometry analysis of TBHP-exposed (500 µM) PC-12 cells demonstrated protection upon the addition of 10 µM ADA-409-052. Data are shown as the averaged green channel (488 nm laser, 530/30 lter) median uorescence intensity (MFI) s.e.m.; = 6/5. Unpaired, two-tailed student's t-test; **p < 0.001. (f) Representative histogram showing the median of the detected green uorescence intensity (log values) a er TBHP treatment only (red) or TBHP and ADA-409-052 (black) using ow cytometry.

æ z v • æ v { x ' " ‡ ˜ ‡ • – • ^ ‡ " " ' ' – ' • ‹ • ‹ • † — … ‡ † „ › Hi h Extracellular con ‡ † ' centrations of glutamate cause GSH-depletion by inhibiting the cysteine/glutamate antiporter system x_c^-[22]. is depletion inhibits GPx4-activity, thereby initiating ferroptosis. Figure 2c,d show that 20 mM glutamate alone resulted in over 90% death of PC-12 cells, while glutamate-exposure in combination with 5, 10, or 20 µM ADA-409-052 rescued more than 90% of the cells (cell survival ADA-409-052: 5 µM: 92.45% 10 µM: 96.2% ± 3.98%, 20 µM: 91.53% ± 2.52%; p < 0.0001, Fig. 2c). In contrast, minocycline was less protective at corresponding concentrations (cell survival minocycline: 10 µM: 24.85% 2%; 20 µM: 49.96% 5.02%; p < 0.0001, Fig. 2d). To demonstrate that the e cacy of ADA-409-052 is independent of endogenous GSH, we determined the intracellular GSH levels in glutamate-exposed PC-12 cells. We found that ADA-409-052 prevented glutamate-exposed cell death e ciently (20 mM Glu: 10.87% 57%; Glu + ADA-409-052: 95.67% ± 0.95%; p < 0.005; Fig. 2e). Also, the GSH levels in both glutamate only and glutamate plus ADA-409-052 co-treated cells were signi cantly reduced compared to unstimulated cells (GSH-levels of: 20 mM Glu 87.8% ADA-409-052: 43.4% 6.3%, unstimulated control cells were normalized to 100%; p < 0.0001, Fig. 2f).

æ z v • æ v { x ' " ‡ ˜ ‡ • – • … Š ƒ • ‰ ‡ • ‹ • • ‹ – ' … Š ' • † " ‹ ƒ Ž • ' " ' Š ' Ž ' ‰ › ‹ • … ‡ Ž Mitochondrial fragmentation is a major morphological alteration in ferroptosis, also when induced by high concentrations of glutamate[23–26]. We thus tested whether ADA-409-052 prevents such changes in mitochondrial morphology of PC-12 cells exposed to ferroptosis stimulation[23]. Live cell imaging of MitoTracker Red CMXRos stained mitochondria showed similar morphology of control, ADA-409-052, as well as glutamate and ADA-409-052-co-treated cells without signs of fragmentation (Fig. 3c,d–g). In contrast, glutamate-exposed cells show clear signs of pronounced fragmentation and reduced mitochondrial density (Fig. 3d,h), comparable with data shown elsewhere[23,26].

æ z v • æ v { x ‹ • Š ‹ „ ‹ – • ‹ • ª ƒ • • f ← " • ‹ • † ‡ Ž ‹ ' • ^ • – ‹ • Lipopolysaccharide (LPS) stimulates in ammatory activation of microglial BV2 cells, which is associated with a redox imbalance. We assessed the expression of inducible nitric oxide synthase (iNOS) by measuring the release of nitric oxide (NO) into the culture medium 24 h a er administration of 50 ng/ml LPS. Co-administration of LPS with ADA-409-052 yielded a dose-dependent reduction in NO release (5 µM: 124.8% 8%; p = 0.0384; 10 µM: 72.33% ± 6.65%, 20 µM: 60.03% ± 9.53%; p < 0.0001; Fig. 4a).

æ z v • æ v { x ‹ • • ‡ — " ' ' " ' – ‡ … – ‹ ˜ ‡ ‹ • ƒ … ' æ … — Ž – — " ‡ • ' † ‡ Ž ' ^ x • ƒ … " ' ' Š ƒ ‰ To determine whether ADA-409-052 protects against in ammation-mediated neuronal death, we exposed co-cultures of N2a cells and RAW 264.7 macrophages to 25 ng/ml LPS and 25-ng/ml interferon gamma (IFN-) for 24 h. e exposure resulted in about 40% neuronal cell death when compared with vehicle treatment (LPS/IFN- : 60.15% 2.28% viability; p < 0.0001). ADA-409-052 improved N2a cell viability

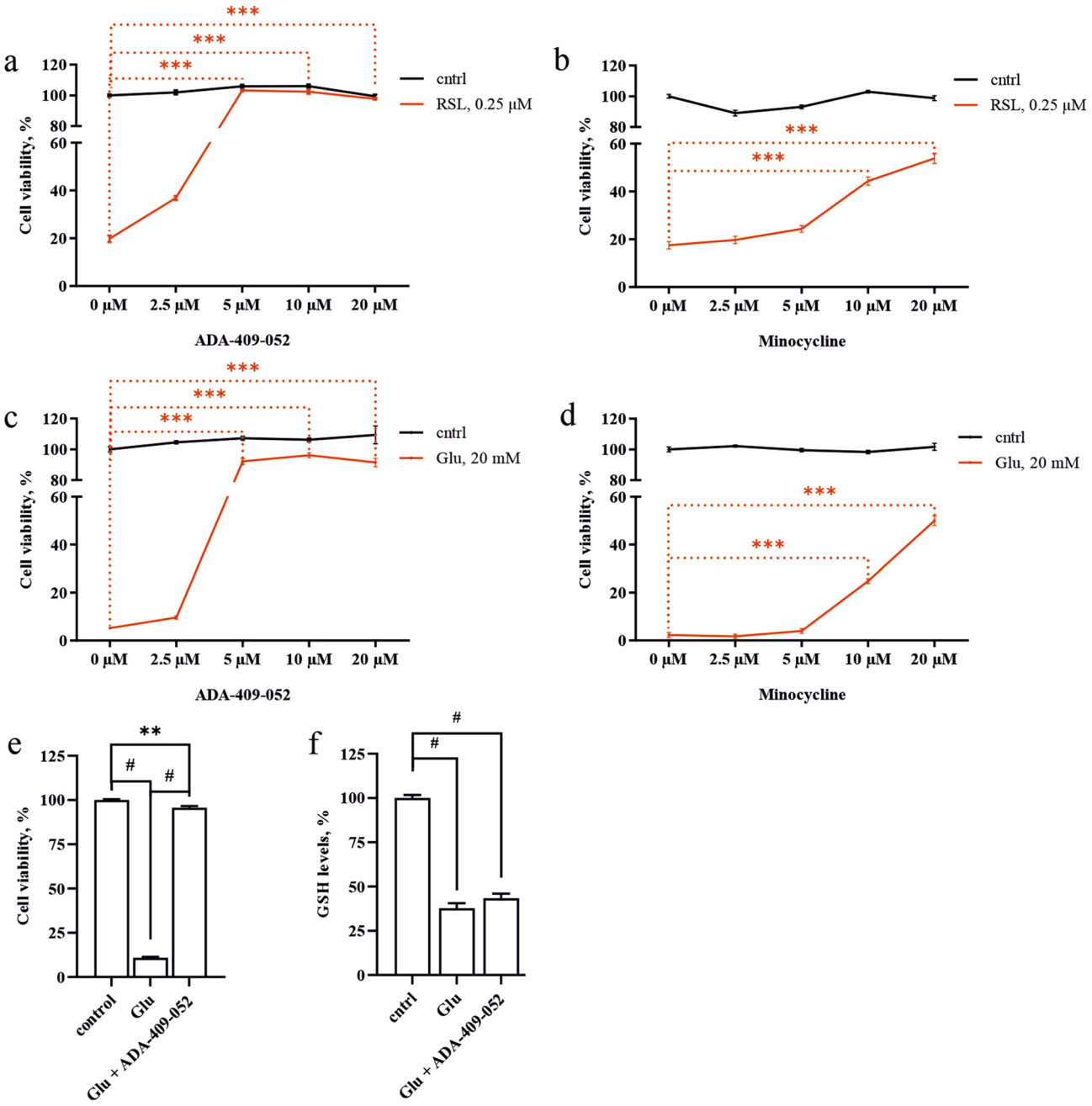

Figure 2. ADA-409-052 is protective against ferroptotic cell death in in vitro models of ferroptosis inducer class I and II. Increased cell viability, detected by the resazurin assay, illustrates the e cacy of ADA-409-052 on cultured PC-12 cells against either RSL3, a class II ferroptosis inducer inactivating GPx4, or glutamate, causing GSH depletion by inhibiting the system x_c^-. (a) ADA-409-052 protects PC-12 cells against RSL3-induced (0.25 µM) ferroptotic cell death signi cantly at all given concentrations (ADA-409-052: 2.5–20 µM). (b) Low concentrations of minocycline (2.5 or 5 µM) were ine cient against RSL3-mediated cell death. However, concentrations of 10 and 20 µM signi cantly improved cell survival. One-way ANOVA followed by Tukey's multiple comparison test; data are presented as percentage mean + SD; n = 3 biological; technical = 6; ***p < 0.0001. (c) ADA-409-052 (5–20 µM) prevented glutamate-induced (20 mM) ferroptotic cell death almost entirely. (d) Minocycline was only protective at concentrations of 10 and 20 µM. One-way ANOVA followed by Tukey's multiple comparison test; data are presented as percentage mean + SD; n = 3 biological; technical = 6; ***p < 0.0001. (e,f) Glutamate-induced reduction of intracellular GSH-levels remains unchanged by ADA-409-052. Exposure of PC-12 cells to glutamate (20 mM) caused a major reduction of cell viability (f) and GSH levels (e) when compared with untreated control cells. While the cell viability was rescued almost entirely by the addition of ADA-409-052 (5 µM), the GSH levels remained comparable to glutamate-exposed cells. One-way ANOVA followed by Tukey's multiple comparison test; data are presented as percentage mean + SD; n = 3 biological; technical = 6; **p = 0.0013; #p < 0.0001.

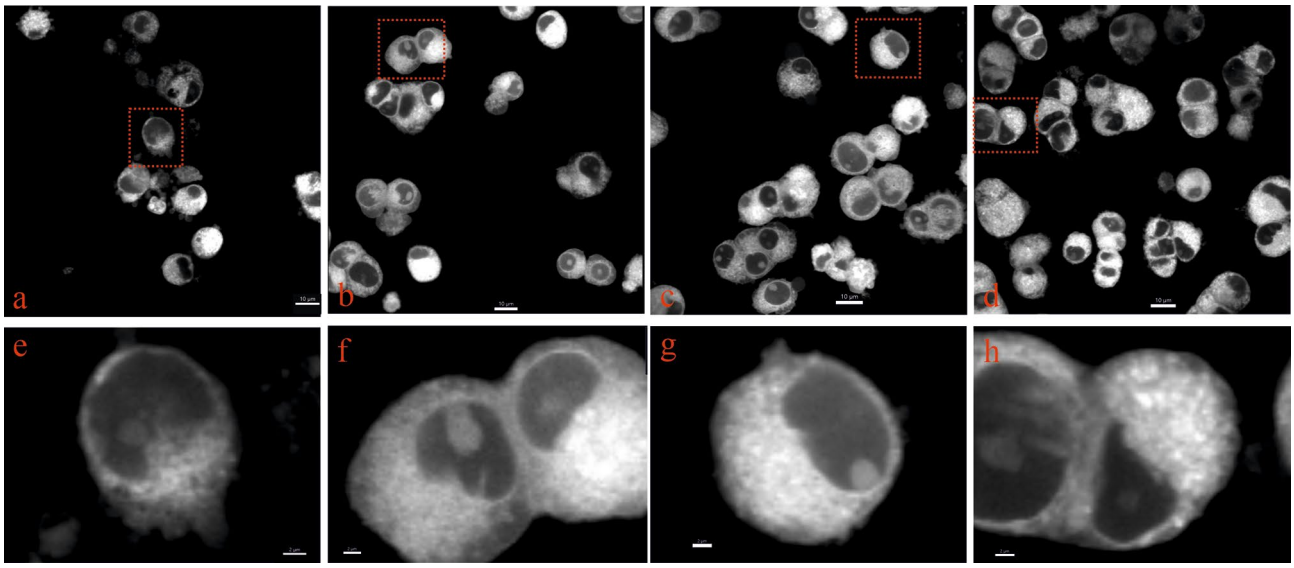

Figure 3. Changes in mitochondrial morphology in glutamate-exposed PC-12 cells are prevented by ADA-409-052. MitoTracker Red CMXRos was used to stain mitochondria of PC-12 cells a er 24 h of exposure to (a,e) 20 mM glutamate, (b,f) glutamate and 10 µM ADA-409-502, or (c,g) ADA-409-052 only, plus control (d,h; media only). (b–d,f–h) Cells, exposed to ADA-409-052 in absence or presence of glutamate show a similar distribution and density of MitoTracker Red CMXRos-positive structures as control cells. (a,e) However, in glutamate-exposed cells appear distribution and density altered, and the overall number of viable cells reduced. Mitochondria were detected by confocal microscopy in live cells and magni ed images (e–h) were produced using Imaris; red boxes indicate magni cations. Scale bar: 10 µm; 2 µm for magni cations.

signi cantly (5 µM ADA-409-052: 64.78 ± 1.77%; $p = 0.0341$), whereas minocycline failed to increase cell sur vival at the same concentration (5 µM minocycline: 61 ± 3.24% cell viability; $p = 0.61$; all Fig. 4b).

æ z v • æ v { x • ' † — Ž ƒ – ‡ • – Š ‡ … › – ' • ‹ • ‡ • ‡ … " ‡ – ‹ ' • ' ^ æ • – ‹ • — ‹ • ˜ ‹ – ' By using the CBA mouse in ammation kit, we determined the e ect of ADA-409-052 on the secretion of pro- and anti-in ammatory cytokines from BV2 cells. e secretion of the anti-in ammatory IL-10 remained unaltered by all used concentrations of ADA-409-052 of BV2 cells (Fig. 4c). However, the addition of 10 µM of the compound reduced the baseline (0 µM ADA-409-052) secretion of MCP-1 by BV2 cells signi cantly (0 µM ADA-409-052: 100 ± 7.43%, 10 µM ADA-409-052: 73.38 ± 5.14%; $p = 0.026$; Fig. 4d). Furthermore, the secretion of TNF- was signi cantly reduced upon exposure to 5 µM when compared with control condition (5 µM ADA-409-052: 69.15 ± 3.24%, $p = 0.042$, Fig. 4e).

" ƒ Ž Ž › ƒ † • ‹ • ‹ • – ‡ " ‡ † æ z v • æ v { x • Š ' ™ • ^ ƒ • – ƒ „ • ' " ' – ‹ ' • Using † ‰ ' ' † a pharmacokinetic study in mice, we established an in vivo treatment protocol. Orally administered ADA-409-052 at the dose of 10 mg/kg showed individual ($n = 3$) maximal plasma concentrations within 0.25–1 h time window, followed by a fast distribution and plasma clearance in a time window of 2–8 h (data not shown). At the 0.75 h time point a er orally dosing 10 mg/kg ADA-409-052, plasma and brain concentrations ($n = 3$) were in the ranges 1080–1324 ng/ml and 1100–1526 ng/g tissue, respectively. Oral administration of 30 mg/kg ADA-409-052 resulted in a mean plasma concentration of 3771 ng/ml and a mean brain concentration of 3237 ng/g at 0.75 h. e concentrations dropped to 23.7 ng/ml and 30.9 ng/g at 4 h, respectively, and below detection limit at 24 h ($n = 3$ per time point). ese results indicated fast and linear dose-dependent oral exposures with excellent brain penetration with a relatively short half-life in the plasma and brain.

" ƒ Ž ƒ † • ‹ • ‹ • – " ƒ – ‹ ' • ' ^ æ z v • æ v { x ' " ' ˜ ‹ † ‡ † ' " ' – ‡ … – ‹ ' • ‹ • æ Š ‡ • ' „ ' Ž ‹ … • – Next, we evaluated whether ADA-409-52 provides neuroprotection in vivo in a TE mouse model of stroke. Minocycline treatment was used as a positive control. ADA-409-052 and minocycline were repeatedly administered post-stroke (Fig. 5a,b). Mice treated with corresponding vehicles were included as negative controls. e oral dosing paradigm of ADA-409-052 was based on our pharmacokinetic study. We dosed minocycline to achieve maximal protection according previous data[27,28]. Quanti cation of the lesion volume by MRI analysis 24 h post-stroke demonstrated a 50% reduction in mice treated with ADA-409-052 when compared to vehicle treatment (ADA-409-052: 10 ± 2.1%, vehicle: 20.5 ± 6.5%; $p = 0.0038$; Fig. 5c). As expected, also minocycline reduced the lesion volume signi cantly when compared to its vehicle treatment (minocycline: 10.3% ± 4.5%, vehicle: 19% ± 8.7%; $p = 0.0319$, Fig. 5c). In addition and importantly, ADA-409-052 attenuated the edematous volume by 39% (ADA-409-052: 5.8 ± 3%, vehicle: 9.2 ± 3.1%; $p = 0.0145$; Fig. 5d), whereas minocycline had no signi cant e ect on brain swelling (minocycline: 5 ± 3.0%, vehicle: 8.5 ± 3.9%; Fig. 5d).

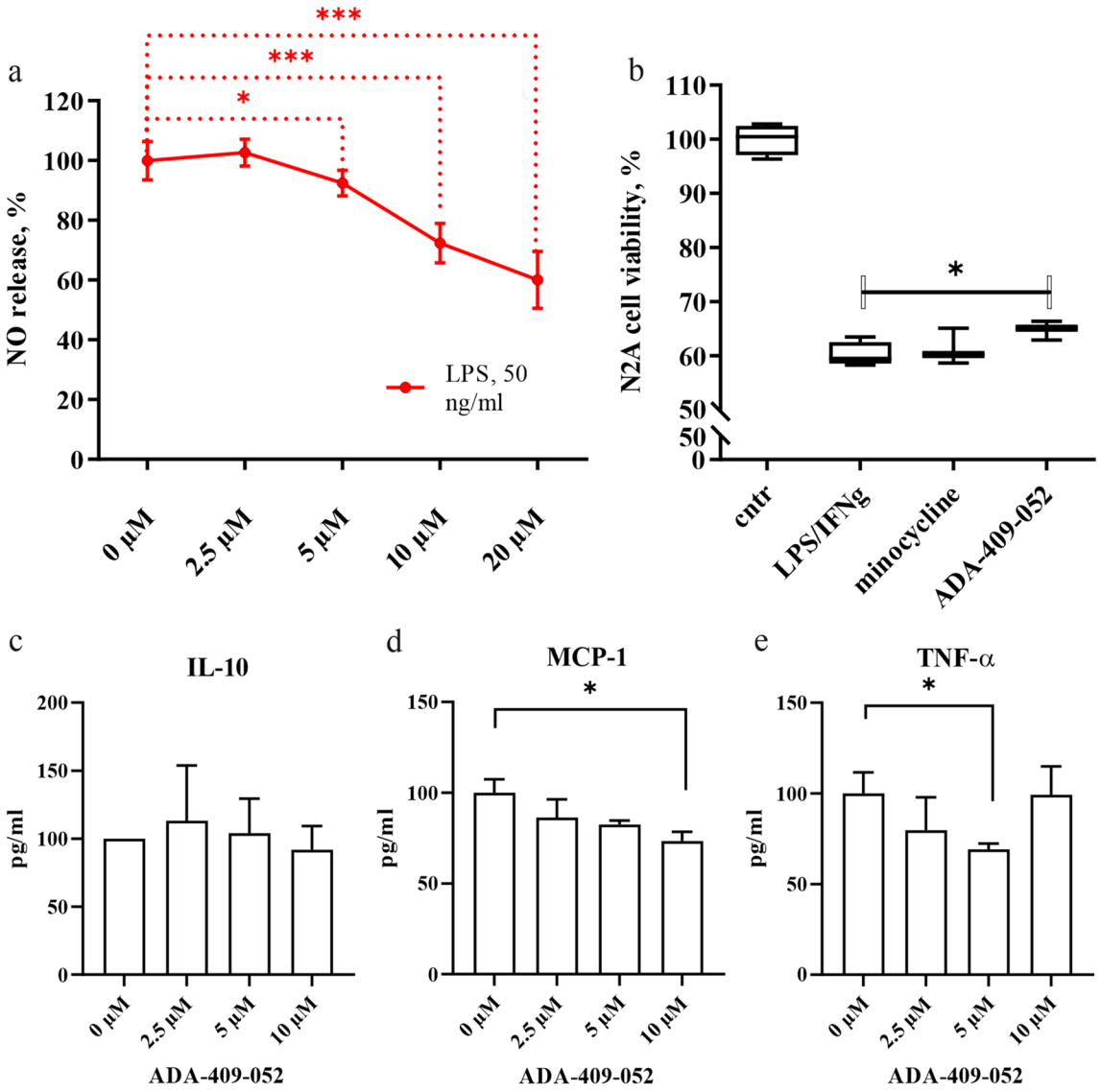

Figure 4. (a) ADA-409-052 inhibits LPS-induced in ammation in BV2 microglial-like cells. e addition of 5, 10, and 20 µM ADA-409-052 signi cantly attenuated the release of NO, measured from the media of LPS-exposed BV2 cells using the Griess reagent, when compared to cells treated with LPS only. Data are represente as percentages of NO-release a er normalization to LPS-stimulated BV2 cells. ; unpaired, two-tailed student's t-test; technical n = 6; *p < 0.05, ***p < 0.0001. (b) ADA-409-052 protects N2a neuronal cells when co-cultured with LPS-stimulated RAW 264.7 macrophages. Boxplots show that LPS and INF- treatment of co-cultured N2a cells and RAW 264.7 macrophages decreased the viability of N2a cells about 40% as detected by the CytoFLEX S (Beckman Coulter) as a fraction of CD11b negative (CD11b), PI negative (PI^-), surviving cells to the total number of gated cells, normalized to the control sample. Co-treatment of ADA-409-052 and LPS/INF- resulted in a signi cant increase of the N2a cell viability, detected by the reduced percentage of CD11b/ PI positive (PI^+, dead) cells when compared to LPS/INF- treatment only. In contrast, the proportion of CD11b/PI^+ N2a cells remained unaltered by minocycline. Cell survival is displayed as individual boxplot per treatment with interquartile range, whiskers set from min to max; unpaired, two-tailed student's t-test; technical n = 3/4; *p = 0.0314. (c–e) ADA-409-052 alters the expression of pro- and anti-in ammatory cytokine expression of BV2 microglial cells. By measuring cytokine-secretion of ADA-409-052-stimulated BV2 cells, using the BD CBA mouse in ammation kit, (c) no changes in secretion of the anti-in ammatory IL-10 were detected. (d) However, we detected a major decrease of MCP-1 upon the addition of 10 µM ADA-409-052. (e) Furthermore, TNF- decreased upon ADA-409-052-stimulation (5 µM) signi cantly when compared with untreated cells (0 µM ADA-409-052). Student's t-test; n = 4; *p<0.05.

a

Treatment	Group size (n)	Dosing	Administration
ADA-409-052	14	100 mg/ kg; 10 ml/ kg	every 4 h, oral gavage in concsiuous mice (p.o.)
Methylcellulose (vehcile)	10	10 ml/ kg	every 4 h, p.o.
Minocycline	15	1st dose: 60 mg/kg; 2nd: 45 mg/ kg	every 12 h, intraperitoneal (i.p.)
0.9% NaCl (saline, vehicle)	13	0,2 ml	every 12 h, i.p.

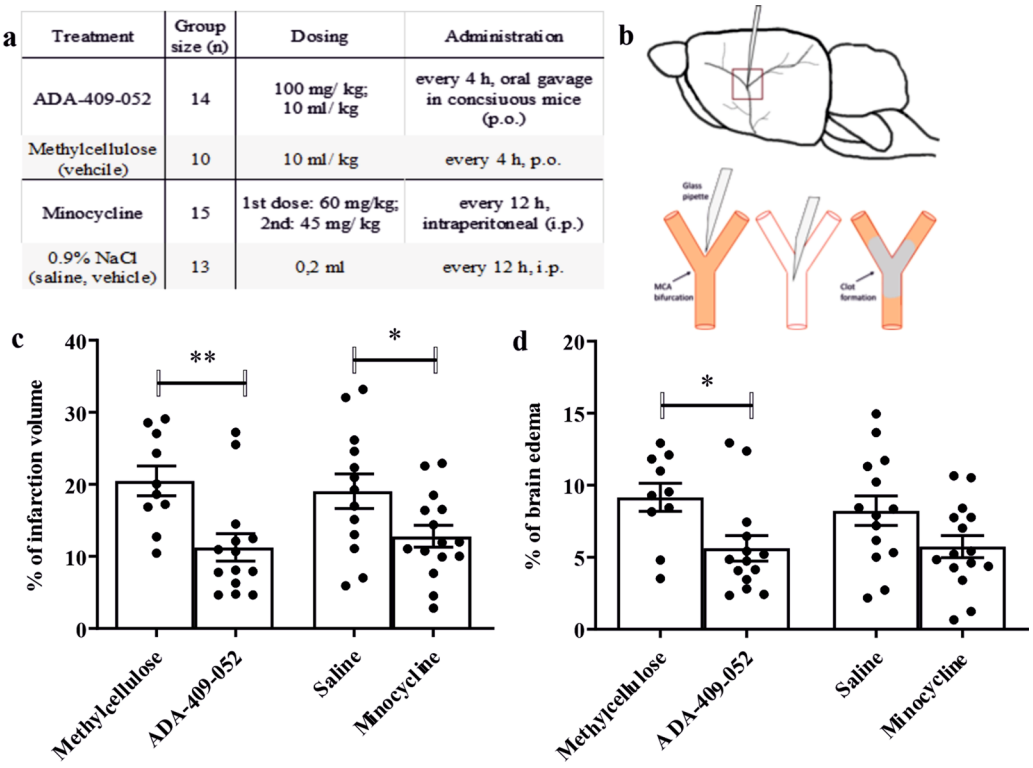

Figure 5. ADA-409-052 administration had a substantial neuroprotective e ect in the TE-mouse model. e table(a) displays the group sizes, drug dosing and administration regime. ADA-409-052 was administered every 4 h, starting -1 h before TE-surgery, with 100 mg/kg at 10 ml/kg p.o. in conscious mice, methylcellulose was given accordingly. Minocycline was injected i.p. as a rst dose of 60 mg/kg and a second dose of 45 mg/kg, every 12 h, whereas 0.2 ml of saline were injected i.p. to the vehicle group. Randomization was done using QuickCalcs (GraphPad So ware). (b) shows a schematic drawing of the MCA-anatomy in the mouse brain, a magni ed view below displays the inserted micropipette, and the in situ clot formation of the murine -thrombin within the MCA (red box indicates the magni ed area). (c,d) ADA-409-052 treatment signi cantly reduced infarct volume and brain edema in mice at 24 h post-ischemic stroke. Minocycline treatment, a competitor compound that was used as positive control, caused a signi cant reduction of the lesion volume. Of note, minocycline failed to reduce the edema size. Lesion and edema volume were assessed using T2-weighted MRI images and calculated according Shuaib's formula[77]. Values are presented as mean ± s.e.m.; unpaired, two-tailed student's t-test; n = 10–15; *p < 0.05; **p < 0.005.

Blood gas levels measured from six randomly selected mice that went through the stroke operation remained unaltered by ADA-409-052 treatment, methylcellulose (vehicle) respectively (data not shown).

æ z v • æ v { x † ‡ … ” ‡ ƒ • ‡ † – Š ‡ ‡ š ’ ” ‡ • • ‹ ‘ • ‘ ^ ’ ” ‘ æ ‹ • ª ƒ • • ƒ – ‘ ” › %
• – ” ‘ • ‡ Stroke is well known to trigger in ammation that contributes to ischemic damage. Since ADA-409-052 provided a mild protection against in ammation-induced neuronal death in vitro, we evaluated whether ADA-409-052 ameliorates ischemia-induced in ammation by analyzing the expression of astrocytic Gfap and allogra in ammatory Aif1 encoding ionized calcium-binding adapter molecule 1 (Iba1), a commonly used microglia marker. Already during the phase of early acute in ammation at 24 h post-stroke, ADA-409-052 suppressed the stroke-induced expression of Gfap in the ipsilateral peri-ischemic area (from 1.059 ± 0.397 to 0.793 ± 0.197; p < 0.05; Fig. 6a), while the expression of Aif1 remained unchanged at the given time point (Fig. 6b). However, in comparison to vehicle-treated mice, ADA-409-052 decreased the mRNA expression of Ccl2 in the ipsilateral perilesional tissue (ADA-409-052 ± 0.294 to vehicle: 10.85 ± 0.584; p = 0.0278; Fig. 6c). Furthermore, the expression of Arg1 (arginase-1) was reduced in the ipsilateral peri-ischemic area of ADA-409-052-treated mice when compared to contralateral peri-ischemic area (ipsilateral: 0.3629 ± 0.3629 vs contralateral: 1.288 ± 0.501; p < 0.001; Fig. 6d). Both compounds reduced the ipsilateral mRNA expression of Il6 significantly in comparison to the contralateral expression (ADA-409-052, ipsilateral: 0.428 ± 0.428 vs contralateral: 1.479 ± 0.396; p < 0.0003; minocycline, ipsilateral: 0.422 ± 0.232 vs contralateral: 0.762 ± 0.375; p < 0.01; Fig. 6e). However, expression of Il10 or Tnf at 24 h post-stroke remained unchanged (data not shown). Interestingly, the expression of Hmox1, encoding for the enzyme heme oxygenase 1 that releases ferrous iron when catabolizing heme, was signi cantly reduced in the ipsilateral peri-ischemic area of ADA-409-052- and minocycline-treated mice compared with the corresponding contralateral expression (ADA-409-052, ipsilateral: 0.368 ± 0.368 vs. contralateral: 1.17 ± 0.33; p = 0.0011; minocycline, ipsilateral: 0.68 ± 0.39 vs. contralateral: 0.96 ± 0.13; p = 0.020

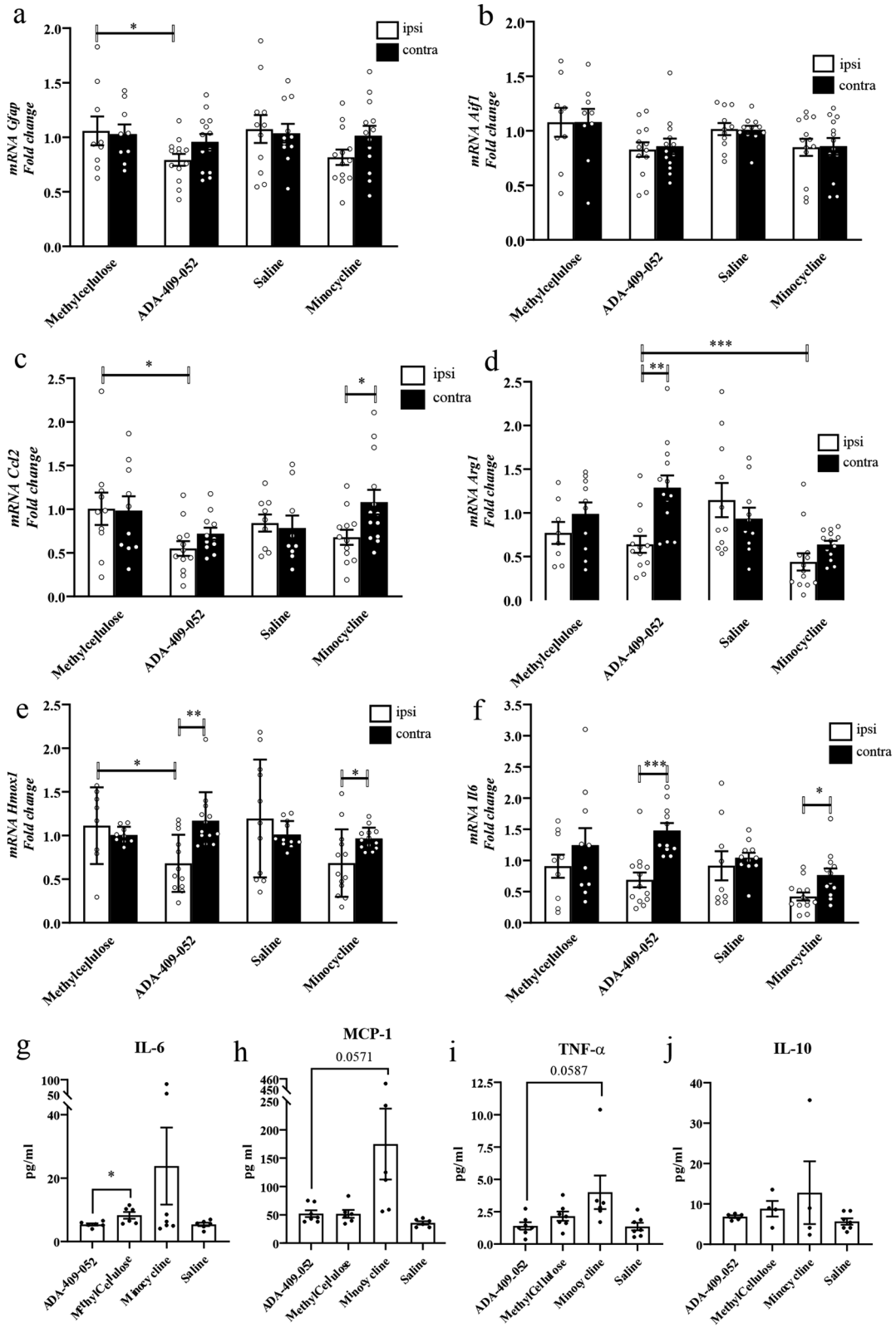
a
mRNA Gfap Fold change
ipsi
contra
Methylcellulose
ADA-409-052
Saline
Minocycline
b
mRNA Aif1 Fold change
c
mRNA Ccl2 Fold change
d
mRNA Arg1 Fold change
e
mRNA Hmox1 Fold change
f
mRNA Il6 Fold change
g
IL-6
pg/ml
h
MCP-1
0.0571
pg ml
i
TNF-α
0.0587
pg/ml
j
IL-10
pg/ml
ADA-409-052
MethylCellulose
Minocycline
Saline

Fig. 6f) and between ADA-409-052- and vehicle-treated control mice (vehicle, ipsilateral: 1.44 ± 0.41; $p = 0.0212$; Fig. 6f).

CBA-analyses of plasma samples, taken at 24 h post-stroke, using the mouse in ammation kit of the BD CBA, revealed signi cantly lower IL-6 levels in mice treated with ADA-409-052 (6.38 ± 0.84 pg/ml) when compared with vehicle-treated mice (8 ± 27.06 pg/ml, $p = 0.027$; Fig. 6g). Although the levels of MCP-1 and TNF- appeared visibly higher in minocycline-treated mice when compared with ADA-409-052-treated mice, the averages remained statistically insigni cant between all treatment groups (Fig. 6h, i). e gene expression data of Il10, however, are in line with the peripheral secretion into the blood plasma of the anti-in ammatory interleukin (Fig. 6j), as both remained unaltered.

‹ • … — • • ‹ ‘ •

e brain is the most susceptible mammalian tissue to the oxidative stress caused by an imbalance of redox reactions. is is due to the brain being extremely rich in lipids with unsaturated fatty acids, which are major substrates for ROS production, while simultaneously consuming about 20% of the oxygen [30]. In addition, most brain areas have a high iron concentration, needed for iron-catalyzed processes, such as oxygen transportation, oxidative phosphorylation, myelin synthesis, and neurotransmitter metabolism [31], leaving the brain sensitive to abnormal iron homeostasis and iron-dependent LP [32]. e risk of unbalanced iron homeostasis and iron-dependent LP is high, especially in the elderly, as iron accumulates into the brain during aging [33]. Moreover, abnormally high iron concentrations are found in a ected brain areas in neurodegenerative diseases, such as AD, PD, amyotrophic lateral sclerosis and

data show that ADA-409-052 suppresses pro-in ammatory activation of microglia- and macrophage-mediated neuronal death. Our ndings are in line with previous studies showing that intracerebral injection of ferrostatin-1, a ferroptosis inhibitor, reduced the expression of COX-2 with concomitant neuroprotection[20]. is indicates that ADA-409-052 and established ferroptosis inhibitors reduce in ammation and in ammation-induced injury also in brain tissue.

To investigate whether the brain penetrating compound ADA-409-052 can provide neuroprotection in vivo, we chose thromboembolic stroke in mice, as this model results in distinct and relatively fast brain injury and